

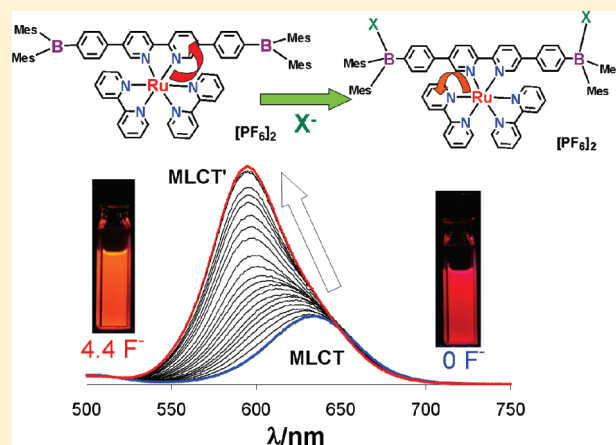
Tuning and Switching MLCT Phosphorescence of $[\text{Ru}(\text{bpy})_3]^{2+}$ Complexes with Triarylboranes and Anions

Yi Sun, Zachary M. Hudson, Yingli Rao, and Suning Wang*

Department of Chemistry, Queen's University, Kingston, Ontario, K7L 3N6, Canada

Supporting Information

ABSTRACT: Four new Ru(II) complexes, $[\text{Ru}(\text{bpy})_2(4,4'\text{-BP2bpy})][\text{PF}_6]_2$ (**1**), $[\text{Ru}(t\text{-Bu-bpy})_2(4,4'\text{-BP2bpy})][\text{PF}_6]_2$ (**2**), $[\text{Ru}(\text{bpy})_2(5,5'\text{-BP2bpy})][\text{PF}_6]_2$ (**3**), and $[\text{Ru}(t\text{-Bu-bpy})_2(5,5'\text{-BP2bpy})][\text{PF}_6]_2$ (**4**) have been synthesized (where $4,4'\text{-BP2bpy}$ = $4,4'\text{-bis}(\text{BMes}_2\text{phenyl})\text{-}2,2'\text{-bpy}$; $5,5'\text{-BP2bpy}$ = $5,5'\text{-bis}(\text{BMes}_2\text{phenyl})\text{-}2,2'\text{-bpy}$ ($4,4'\text{-BP2bpy}$); and $t\text{-Bu-bpy}$ = $4,4'\text{-bis}(t\text{-butyl})\text{-}2,2'\text{-bipyridine}$). These new complexes have been fully characterized. The crystal structures of **3** and **4** were determined by single-crystal X-ray diffraction analyses. All four complexes display distinct metal-to-ligand charge transfer (MLCT) phosphorescence that has a similar quantum efficiency as that of $[\text{Ru}(\text{bpy})_3][\text{PF}_6]_2$ under air, but is at a much lower energy. The MLCT phosphorescence of these complexes has been found to be highly sensitive toward anions such as fluoride and cyanide, which switch the MLCT band to higher energy when added. The triarylboron groups in these compounds not only introduce this color switching mechanism, but also play a key role in the phosphorescence color of the complexes.



INTRODUCTION

Conjugated three-coordinate organoboron compounds have recently emerged as an important class of photonic and optoelectronic materials, for use in applications such as nonlinear optics¹ and as charge-transport and emissive materials in organic light-emitting diodes (OLEDs).² Furthermore, three-coordinate organoboron compounds have also been shown to be effective colorimetric, fluorescent, ratiometric, or electrochemical sensors for the selective detection of anions such as fluoride and cyanide, via disruption of the $p_\pi\text{--}\pi$ conjugation around the boron center.^{3–6} Functionalization of metal complexes by a triarylboron group has been found recently to enhance the affinity of the boron center to anions,^{5,6} as well as the phosphorescence or electrophosphorescence of the complexes.⁷ Previously, we reported that the attachment of BMes_2 groups to a $2,2'\text{-bpy}$ ($2,2'\text{-bpy}$ = $2,2'\text{-bipyridine}$) core at the 5 and 5' positions, or to a $2,2'\text{-bpy}$ core through a phenyl linker at either the 5,5' or 4,4' positions can have a significant impact on MLCT energy, phosphorescence, and the affinity to anions of their Pt(II) and Cu(I) compounds.⁵ Because of the importance of Ru(II)-bpy complexes in photochemistry and their distinct metal-to-ligand charge transfer (MLCT) transitions,⁸ we have now extended our study to ruthenium(II) complexes to examine the impact of the triarylboron-functionalized bpy ligands $5,5'\text{-bis}(\text{BMes}_2\text{phenyl})\text{-}2,2'\text{-bpy}$ ($5,5'\text{-BP2bpy}$) or $4,4'\text{-bis}(\text{BMes}_2\text{phenyl})\text{-}2,2'\text{-bpy}$ ($4,4'\text{-BP2bpy}$) on the MLCT transitions and phosphorescence of these compounds. We have observed that compared to the parent complex⁸ $[\text{Ru}(\text{bpy})_3]^{2+}$, the triarylboron

unit significantly shifts the MLCT phosphorescence energy and makes this emission band switchable via the addition of anions.

RESULTS AND DISCUSSION

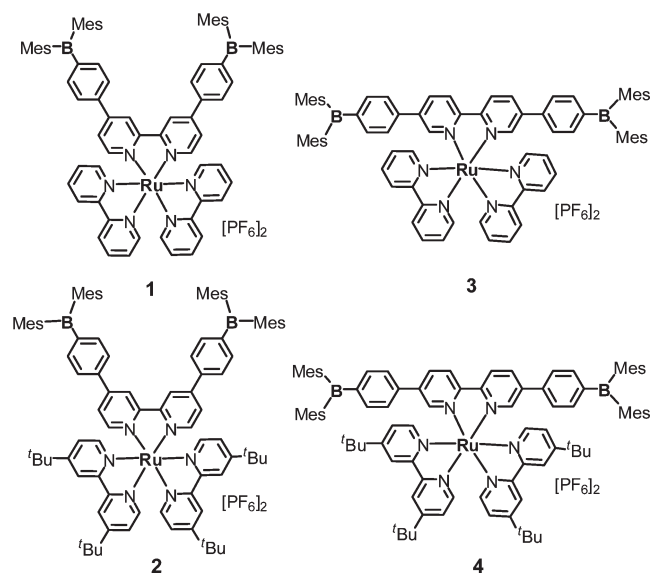
Synthesis and Structures. The bpy derivatives $5,5'\text{-BP2bpy}$ and $4,4'\text{-BP2bpy}$ were prepared according to our previous report.^{5c} The synthesis of the ruthenium complexes **1–4** (where **1** is $[\text{Ru}(\text{bpy})_2(4,4'\text{-BP2bpy})][\text{PF}_6]_2$, **2** is $[\text{Ru}(t\text{-Bu-bpy})_2(4,4'\text{-BP2bpy})][\text{PF}_6]_2$, **3** is $[\text{Ru}(\text{bpy})_2(5,5'\text{-BP2bpy})][\text{PF}_6]_2$, and **4** is $[\text{Ru}(t\text{-Bu-bpy})_2(5,5'\text{-BP2bpy})][\text{PF}_6]_2$) were achieved by refluxing the chelate ligands with $\text{cis-Ru}(\text{bpy})_2\text{Cl}_2$ and $\text{cis-Ru}((2,2'\text{-bis}(4\text{-}t\text{-Bu})\text{-bpy})_2\text{Cl}_2$, respectively, in ethanol under nitrogen, followed by an anion exchange of chloride with PF_6^- . The structures of the four new Ru(II) complexes are shown in Chart 1.

The new complexes all have a deep red-orange or red color and have been fully characterized by NMR spectroscopy and elemental analysis. The crystal structures of **3** and **4** were determined by single-crystal X-ray diffraction analysis and both display similar structures. The structure of the cation of **3** is shown in Figure 1. The structure of **4** can be found in the Supporting Information. The crystal structures of **3** and **4** confirm the presence of a somewhat-distorted octahedral geometry around the Ru(II) center. The Ru–N bond distances in **3** are in the range of

Received: November 1, 2010

Published: March 17, 2011

Chart 1



2.049(4)–2.069(1) Å, with *trans* N–Ru–N angles of 168.96(14)°–173.34(15)°. Similar bond lengths and angles were also observed for compound 4. The two phenyl rings on the 5,5'-BP2bpy ligand have dihedral angles of 46.0° and 96.5° with the bpy ring, attributable to steric interactions. The cation of 3 displays extensive interaction π -stacking between the bpy rings and the mesityl groups, forming an extended two-dimensional (2D) array with the shortest atomic contact distance being 3.33 Å. In contrast, the cation of 4 forms a discrete π -stacked dimer through the interactions between the 5,5'-BP2bpy ligands from two neighboring cations, and these dimers are separated from each other by the counterions (see Figure 1).

Absorption and Luminescence Spectra. The absorption and luminescence data of 1–4, along with those of $[\text{Ru}(\text{bpy})_3]^{2+}$, are summarized in Table 1. As shown in Figure 2, the absorption spectra of 1 and 2 resemble each other but are distinctly different from those of 3 and 4. For 3 and 4, there are intense bands at 370 and 361 nm, respectively, that can be assigned to the 5,5'-BP2bpy chromophore. For 1 and 2, these bands appear as a shoulder peak and at a higher energy.

The lowest energy absorption band in all four compounds is a broad metal-to-ligand-charge-transfer (MLCT) band, from ~400 nm to 500 nm, that appears at a lower value than that of the parent molecule $[\text{Ru}(\text{bpy})_3][\text{PF}_6]_2$. The molar extinction coefficients of the MLCT bands for the boron-functionalized complexes of 1 and 2 are much higher than those of 3, 4, and $\text{Ru}(\text{bpy})_3[\text{PF}_6]_2$. This appears to support the belief that the 4,4'-BP2bpy ligand is much more effective in facilitating the MLCT transition, perhaps because of a relatively large dipole (*t*-butyl-bpy to 4,4'-BMes2), compared to 5,5'-BP2bpy. Complexes 1–4 are all luminescent in solution and the solid state at ambient temperature (see Figure 2). In air, the phosphorescence quantum efficiencies and decay lifetimes of 1–4 are similar to those of $[\text{Ru}(\text{bpy})_3][\text{PF}_6]_2$, as shown in Table 1. The emission is phosphorescent in nature as it experiences a significant reduction in intensity upon exposure to air. Nonetheless, all four compounds display appreciable phosphorescent efficiency in air, as shown in Table 1. Since MLCT is clearly the lowest-energy

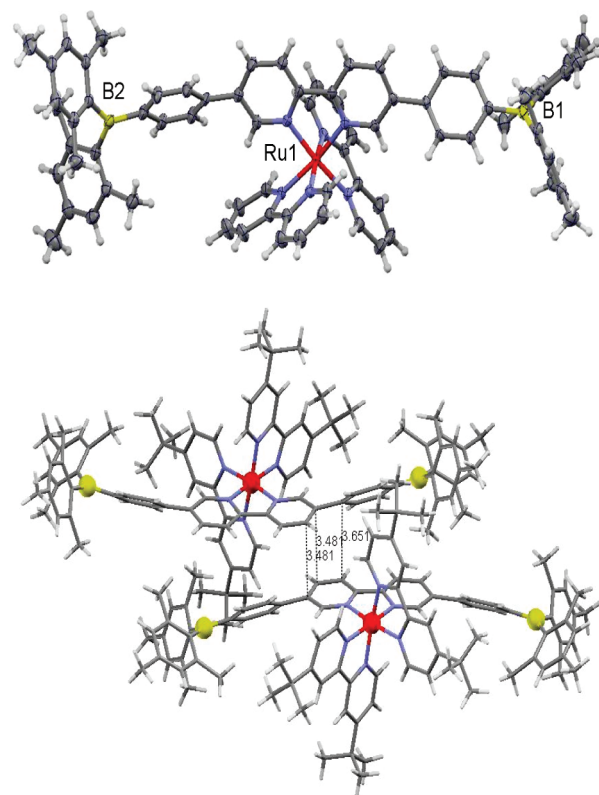


Figure 1. (Top) The structure of the cation of compound 3 with 35% ellipsoids. (Bottom) A diagram showing the π -stacked dimer of the cation of 4.

excited state, the phosphorescence of these molecules is attributed to MLCT transitions, according to Kasha's rule.¹⁰ The phosphorescence energy of the boron-functionalized Ru(II) complexes is red-shifted in all cases, compared to that of $[\text{Ru}(\text{bpy})_3]^{2+}$, by as much as 35 nm (compound 4), which is an indication that the MLCT emission likely involves the boron-functionalized bpy, since the electron-accepting nature of the triarylboron group and the greater π -conjugation of the boron-functionalized bpy can effectively lower the LUMO energy, thus decreasing the energy of the MLCT excited state. The MLCT emission can be thus assigned to $\text{Ru} \rightarrow \text{BP2bpy}$. The two *t*-butyl-bpy complexes 2 and 4 have lower phosphorescence energies than those of the bpy complexes 1 and 3. This may be explained by the electron-donating *t*-butyl groups, which increase the HOMO (t_{2g}) energy level, thus decreasing the optical band gap. Thus, the observed variation of the MLCT phosphorescence energy in 1–4 can be considered to be the result of a combined perturbation of the BMes₂ group on the LUMO (π^*) and the *t*-butyl on the HOMO (t_{2g}) orbitals, as frequently observed for substituted Ru(II)-bpy complexes.⁸ DFT and TD-DFT computations were performed for the dications of 1–4, in order to validate the origin of the phosphorescence emission. However, despite the use of commonly used methods and basis sets for previous studies on Ru(II) compounds,¹¹ the results failed to capture significant Ru(II) *d* character in the HOMO to HOMO–8, giving only ligand-centered transitions as a result. Therefore, these results cannot be considered to be meaningful, because both voltammetric and spectroscopic data indicate clear participation of Ru(II) in the HOMO levels, and future studies may require the use of an alternative computational approach.

Table 1. Absorption and Luminescence Data

complex	UV-vis, nm (ϵ , M ⁻¹ cm ⁻¹)	Data for CH ₂ Cl ₂ @ 298 K		Data for CH ₂ Cl ₂ @ 77 K	
		λ_{em} , nm	λ_{em} , nm	τ , ^a μ s	ϕ ^b
Ru(bpy) ₃ ²⁺	455 (14 000)	600	585	3.7(1)	0.016
1	345 (45 600), 466 (24 800)	604	595	6.2(2)	0.018
2	333 (41 900), 475 (21 100)	624	612	4.2(1)	0.019
3	370 (65 900), 457 (12 800)	616	606	5.8(2)	0.017
4	361 (59 200), 458 (11 300)	631	620	3.5(1)	0.020

^a Decay lifetimes were measured under N₂ at 77 K. ^b The quantum efficiencies for the Ru(II) complexes were measured using [Ru(bpy)₃][PF₆]₂ as the reference in CH₂Cl₂ under air. The quantum efficiency of [Ru(bpy)₃][PF₆]₂ under nitrogen has been reported to be 0.029 in CH₂Cl₂.⁹

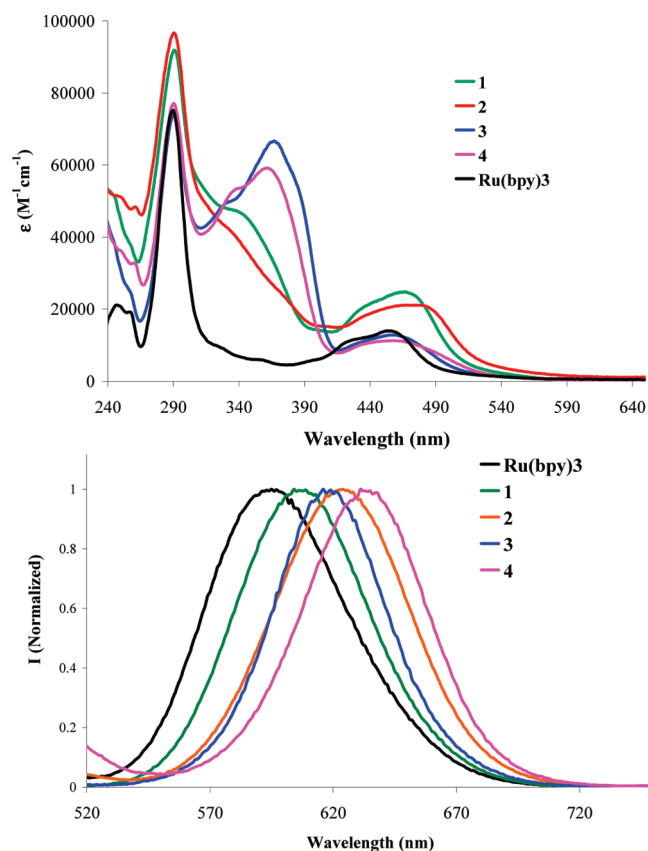


Figure 2. UV-vis (top) and phosphorescent (bottom) spectra of 10⁻⁵ M solutions of Ru(II) complexes recorded in CH₂Cl₂.

Electrochemical Properties. The electrochemical redox properties of Ru(II) complexes were recorded by cyclic voltammetry (CV). Compounds 1–4 all exhibit multiple reduction waves, which can be attributed to the sequential reduction of the bpy chelate, the BP2bpy chelate, and the boron centers. As shown in Figure 3 and Table 2, the first reduction peak for the Ru(II) complexes was observed at –1.74 V (1), –1.76 V (2), –1.59 V (3), and –1.60 V (4) versus FeCp₂^{0/+}, respectively. The 5,5'-BP2bpy compounds 3 and 4 have the most-positive first reduction potential, indicating a greater electronic impact of chelation on 5,5'-B2bpy than 4,4'-B2bpy. To examine the impact of the BMe₂ groups on the Ru^{II/III} redox couple, the CV diagram of the nonborylated complex, [Ru(bpy)₃][PF₆]₂ was recorded and compared under the same conditions. This complex has the most-negative reduction potential at –1.85 V, compared to the new borylated complexes, supporting

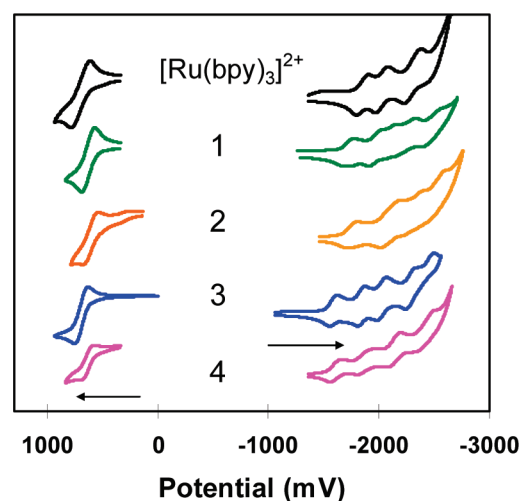


Figure 3. Cyclic voltammetry (CV) diagrams for all Ru complexes recorded in DMF, showing the oxidation and reduction peaks. The potential is relative to that of FeCp₂^{0/+}.

the belief that the boron center lowers the LUMO energy and enhances the electron affinity of the molecule. In addition, the reduction potentials of the borylated complexes are all much more positive than those of the free ligands, supporting the belief that chelation by Ru(II) enhances the electron-accepting ability of the ligands. This is consistent with our earlier observations for Pt(II) and Cu(I) complexes.^{5c} All Ru(II) complexes display one reversible oxidation wave that can be assigned to the Ru(II)/Ru(III) couple. The oxidation potential of 1, 2, and 4 is somewhat less positive than that of Ru(bpy)₃²⁺, indicating the increase of the HOMO level. For 2 and 4, the electron-donating *t*-butyl groups may be responsible for this. It is unclear why the HOMO of 1 is higher than that of Ru(bpy)₃²⁺. Using the CV data, the electrochemical energy gaps of 1–4 were calculated, which are all smaller than that of Ru(bpy)₃²⁺ (Table 2), in agreement with the red shift of the emission spectra of 1–4, compared to Ru(bpy)₃²⁺.

Switching MLCT Energy with Fluoride and Cyanide Ions. To further confirm the involvement of the triarylboron group in the MLCT phosphorescence of 1–4, we examined the UV-vis and phosphorescence spectral changes of these complexes upon the addition of fluoride (NBu₄F) in CH₂Cl₂. For 2 and 4, titration with cyanide (NEt₄CN) in CH₂Cl₂ was also performed. The titration data are shown in Figures 4 and 5 for fluoride. The cyanide behaves very similarly to fluoride for 2 and 4 with similar spectral change. Its titration spectra can be found in the Supporting Information. The addition of fluoride and cyanide ions caused a

Table 2. Electrochemical Data^a

	$E_{1/2}^{\text{red1}}$ (V)	$E_{1/2}^{\text{red2}}$ (V)	$E_{1/2}^{\text{red3}}$ (V)	$E_{1/2}^{\text{red3}}$ (V)	$E_{1/2}^{\text{ox}}$ (V)	electrochemical energy gap (V)
$\text{Ru}(\text{bpy})_3^{2+}$	−1.85	−2.03	−2.31		0.70	2.58
1	−1.74	−1.97	−2.24	−2.48	0.63	2.37
2	−1.76	−2.10	−2.31	−2.53	0.61	2.37
3	−1.59	−1.84	−2.03	−2.29	0.69	2.28
4	−1.60	−1.87	−2.13	−2.42	0.64	2.24
4,4-BP2bpy ^b	−2.05	−2.48				
5,5'-BP2bpy ^b	−2.04	−2.67				

^a All potentials are relative to $\text{FcP}_2^{0/+}$, measured in DMF, using NBu_4PF_6 as the electrolyte with a scan rate of 25 mV to 200 mV. ^b Reference 5c.

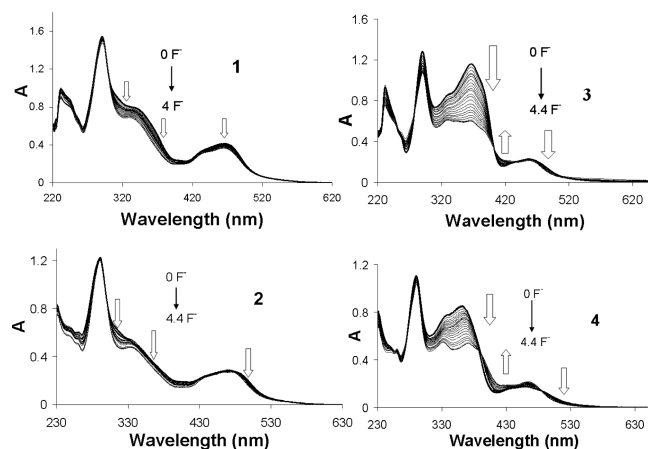


Figure 4. UV-vis spectral change of complexes **1–4** with the addition of NBu_4F in CH_2Cl_2 .

decrease of the boryl absorption band at ~ 350 nm, and a slight decrease and blue shift of the MLCT absorption band. The most distinct change was observed in the phosphorescence spectra. As shown in Figure 5, the addition of fluoride or cyanide generally switches the emission energy of the complex to higher energy, changing color from red to orange. In addition, except for **1**, which experiences some decrease in emission intensity with anion addition, all complexes significantly gain phosphorescence intensity. The high sensitivity of the MLCT phosphorescence band toward anions confirms the involvement of the boryl group in the MLCT transition. The phosphorescence energy switching from low energy to high energy is in agreement with the change of the boryl group from electron-withdrawing to electron-donating with anion binding. Furthermore, the emission energy of all the fluoride adducts appears at $\lambda_{\text{max}} \approx 585\text{--}600$ nm, which resembles that of $\text{Ru}(\text{bpy})_3^{2+}$ and is much lower in energy than the BP2bpy-centered triplet state.^{5c} Thus, it may be described that anion binding in this system switches MLCT phosphorescence from a primarily $\text{Ru} \rightarrow \text{BP2bpy}$ transition to a $\text{Ru} \rightarrow \text{bpy}$ transition. The emission intensity variation upon anion binding in this system is not well understood. The enhancement in **2–4** may be explained by the fact that the $\text{Ru} \rightarrow \text{BP2bpy}$ emission is switched to a much higher energy of $\text{Ru} \rightarrow \text{bpy}$ emission (a 25–40 nm shift). Thus, based on the energy gap law, less energy loss via nonradiative decay process occurs. In contrast, the emission energy change in **1** is much less (10 nm). The overall binding constants for the $\text{Ru}(\text{II})$ complexes with F^- were estimated to be in the range of $\sim 7 \times 10^8 \text{ M}^{-2}$ to $2 \times 10^9 \text{ M}^{-2}$ (see the Supporting Information); these values are similar to those

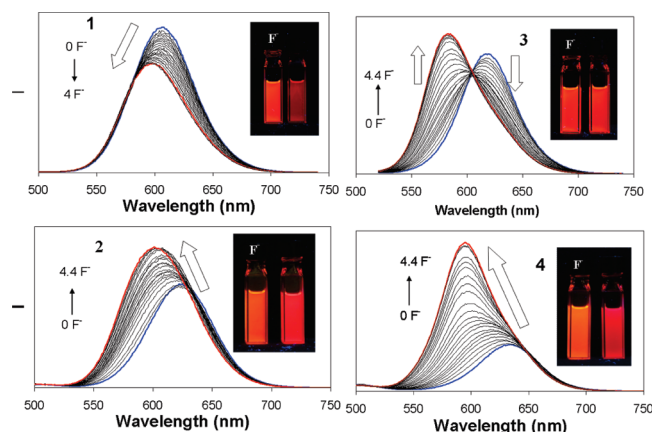


Figure 5. Phosphorescence titration diagrams of **1–4** with the addition of NBu_4F in CH_2Cl_2 . Inset: Photographs showing the color change before fluoride addition (right) and after fluoride addition (left).

of PtPh_2 complexes that contain the same boryl ligands.^{5c} For **2**, the binding constants with F^- and CN^- are similar ($2 \times 10^9 \text{ M}^{-2}$ and $1 \times 10^9 \text{ M}^{-2}$, respectively). For **4**, ^{11}B NMR competition experiments indicate slightly stronger binding to CN^- , as the CN^- and F^- adducts are formed in an approximately 3:1 ratio when these complexes are treated simultaneously with 2 equiv of both anions, which also agrees with the phosphorescent titration data. Fluoride and cyanide sensing in absorption mode, using a cyclometalated $\text{Ru}(\text{II})$ complex, has been recently reported by Gabbai and co-workers, where cyanide was found to have a stronger binding than fluoride.^{6f} Our compounds are the first examples that demonstrate the switching of MLCT phosphorescence using fluoride or cyanide in a $\text{Ru}(\text{II})$ compound.

In conclusion, four new ruthenium(II) complexes based on the two diboryl 5,5'-biphenyl-2,2'-bpy or 4,4'-biphenyl-2,2'-bpy ligands have been achieved. These complexes display distinct MLCT transition bands and phosphorescence that are dependent on the geometry of the bis-boryl chelate ligands. The boryl group has been found to lower the LUMO level, thus enhancing the electron-accepting ability of the complex. The MLCT phosphorescence of these new $\text{Ru}(\text{II})$ complexes is highly sensitive to fluoride and cyanide binding, which provides a convenient method for sensing these anions, and tuning the MLCT emission energy of the metal complexes.

EXPERIMENTAL SECTION

General. All reactions were performed under dry N_2 with standard Schlenk techniques unless otherwise noted. All starting materials were purchased from Aldrich Chemical Co. and used without further

purification. Deuterated solvents CDCl_3 and CD_2Cl_2 (Cambridge Isotopes) were used as received without further drying. NMR spectra were recorded on a Bruker Avance 400 spectrometer (400.13 MHz for ^1H , 100.62 MHz for ^{13}C). UV–vis spectra were recorded on an Ocean Optics ISS-UV–vis spectrophotometer. Excitation and emission spectra were recorded on a Photon Technologies International QuantaMaster model C-60 spectrometer. Emission lifetimes were measured on a Photon Technologies International phosphorimeter (Time-Master C-631F) that was equipped with a xenon flash lamp and a digital-emission photon multiplier tube, using a band pathway of 5 nm for excitation and 2 nm for emission. Cyclic voltammetry (CV) was performed using a BAS CV-50W analyzer, with a scan rate of 25 mV/s to 200 mV/s and a typical concentration of 5 mg of the compound in 2 mL of DMF, at room temperature using 0.10 M NBu_4PF_6 as the supporting electrolyte. The electrolytic cell used was a conventional three-compartment cell, in which a Pt working electrode, a Pt auxiliary electrode, and an Ag/AgCl reference electrode were employed. The ferrocenium/ferrocene couple was used as the internal standard ($E_0 = 0.662$ V). Elemental analyses were performed at Canadian Microanalytical Service, Ltd. (Delta, British Columbia, Canada). DFT calculations were carried out using the LANL2DZ pseudopotential for Ru, and 6-31 g(d) as the basis set for all other atoms. Crystal structures were used as the starting point for geometry optimizations where possible. $5,5'$ -(*p*-Bmes₂-phenyl)₂-2,2'-bpy ($5,5'$ -BP2bpy) and $4,4'$ -(*p*-Bmes₂-phenyl)₂-2,2'-bpy ($4,4'$ -BP2bpy) were prepared using methods described in the literature.^{5c}

[(2,2'-bpy)₂Ru(4,4'-BP2bpy)][PF₆]₂ (1). A solution of *cis*-dichlorobis(2,2'-bipyridyl)ruthenium(II) (52 mg, 0.10 mmol) and $4,4'$ -BP2bpy (80 mg, 0.10 mmol) in 10 mL of ethanol was stirred under reflux for 48 h under nitrogen. After cooling to room temperature, the solution was concentrated under reduced pressure and treated with a saturated aqueous solution of NH_4PF_6 , which gave a red precipitate. The crude product was then purified by column chromatography (silica gel, eluted with CH_3OH : $\text{CH}_2\text{Cl}_2 = 1: 20$, v/v). Red solid was obtained in 46% yield. ^1H NMR (400 MHz, CD_2Cl_2): 8.63 (d, $J = 1.2$ Hz, 2H, H_1), 8.45 (d, $J = 8.0$ Hz, 4H, H_6), 8.08 (m, 4H, H_7), 7.85 (d, $J = 4.8$ Hz, 2H, H_3), 7.78–7.75 (m, 8H, $H_9 + H_5$), 7.71 (dd, $J = 4.8$ Hz, $J = 1.2$ Hz, 2H, H_2), 7.64 (d, $J = 8.4$ Hz, 4H, H_4), 7.49 (m, 4H, H_8), 6.85 (s, 8H, H of Mes), 2.31 (s, 12H, CH_3 of Mes), 1.99 (s, 24H, CH_3 of Mes). ^{13}C NMR (100 MHz, CD_2Cl_2): 168.9, 157.2, 157.0, 150.4, 148.8, 141.7, 141.1, 139.6, 138.7, 138.5, 138.4, 137.9, 136.7, 136.6, 129.3, 127.9, 126.9, 126.7 (aryl C), 23.5, 21.7 (CH_3 of Mes). Anal. Calcd for $\text{C}_{78}\text{H}_{74}\text{B}_2\text{F}_{12}\text{N}_6\text{P}_2\text{Ru}$: C, 62.12; H, 4.95; N, 5.57. Found: C, 62.36; H, 5.15; N, 5.36.

[(2,2'-*t*-Bu₂bpy)₂Ru(4,4'-BP2bpy)][PF₆]₂ (2). The complex was synthesized using the same method as that applied for complex 1. Red solid was obtained in 52% yield. ^1H NMR (400 MHz, CD_2Cl_2): 8.62 (d, $J = 1.2$ Hz, 2H, H_1), 8.29 (d, $J = 1.2$ Hz, 4H, H_6), 7.79–7.77 (m, 6H, $H_3 + H_5$), 7.73 (dd, $J = 4.0$ Hz, $J = 1.2$ Hz, 2H, H_2), 7.71 (d, $J = 4.0$ Hz, 2H, H_8), 7.65 (d, $J = 5.6$ Hz, 4H, H_4), 7.49 (dd, $J = 2.0$ Hz, $J = 6.0$ Hz, 2H, H_7), 6.85 (s, 8H, H of Mes), 2.30 (s, 12H, CH_3 of Mes), 1.98 (s, 24H, CH_3 of Mes), 1.43 (s, 18H, H of *t*-Bu), 1.36 (s, 18H, H of *t*-Bu). ^{13}C NMR (100 MHz, CD_2Cl_2): 162.9, 159.6, 157.4, 156.8, 156.7, 152.0, 151.1, 149.7, 148.6, 141.7, 141.0, 139.5, 138.9, 137.3, 128.6, 127.1, 125.8, 122.7, 121.7, 121.6, 120.9, 117.4 (aryl C), 35.8, 30.3, 30.2 (*t*-Bu), 23.5, 21.7 (CH_3 of Mes). Anal. Calcd for $\text{C}_{94}\text{H}_{106}\text{B}_2\text{F}_{12}\text{N}_6\text{P}_2\text{Ru}$: C, 65.71; H, 6.17; N, 4.85. Found: C, 65.75; H, 6.50; N, 5.01.

[(2,2'-bpy)₂Ru(5,5'-BP2bpy)][PF₆]₂ (3). The complex was synthesized using the same method as that applied for complex 1. Red solid was obtained in 39% yield. ^1H NMR (400 MHz, CD_2Cl_2): 8.57 (d, $J = 8.4$ Hz, 2H, H_3), 8.45 (t, $J = 8.4$ Hz, 4H, H_6), 8.35 (d, $J = 8.4$ Hz, H_2), 8.08 (m, 4H, H_7), 7.88 (s, 2H, H_1), 7.84 (d, $J = 3$ Hz, 2H, H_9), 7.78 (d, $J = 3$ Hz, 2H, H_5), 7.53 (d, $J = 7.2$ Hz, 4H, H_4), 7.49 (m, 4H, H_8), 7.33 (d, $J = 7.2$ Hz, 4H, H_4), 6.83 (s, 8H, H of Mes), 2.30 (s, 12H, CH_3 of Mes), 1.98 (s, 24H, CH_3 of Mes). ^{13}C NMR (100 MHz, CD_2Cl_2): 171.1, 157.2,

156.8, 155.6, 151.8, 148.5, 147.8, 141.6, 141.0, 140.3, 139.5, 138.7, 138.6, 137.5, 137.0, 136.5, 128.7, 128.6, 128.5, 126.5, 125.0, 124.8, 124.4 (aryl C), 23.5, 21.2 (CH_3 of Mes). Anal. Calcd for $\text{C}_{78}\text{H}_{74}\text{B}_2\text{F}_{12}\text{N}_6\text{P}_2\text{Ru}$: C, 62.12; H, 4.95; N, 5.57. Found: C, 62.17; H, 5.08; N, 5.40.

[(2,2'-*t*-Bu₂bpy)₂Ru(5,5'-BP2bpy)][PF₆]₂ (4). The complex was synthesized using the same method as that applied for complex 1. Red solid was obtained in 48% yield. ^1H NMR (400 MHz, CDCl_3): 8.57 (d, $J = 8.4$ Hz, 2H, H_3), 8.31–8.28 (m, 6H, $H_2 + H_6$), 7.72 (m, 6H, $H_1 + H_8$), 7.54–7.47 (m, 8H, $H_5 + H_7$), 7.33 (d, $J = 8.4$ Hz, 4H, H_4), 6.84 (s, 8H, H of Mes), 2.31 (s, 12H, CH_3 of Mes), 1.96 (s, 24H, CH_3 of Mes), 1.42 (s, 18H, H of *t*-Bu), 1.36 (s, 18H, H of *t*-Bu). ^{13}C NMR (100 MHz, CD_2Cl_2): 163.4, 157.2, 156.8, 156.1, 151.6, 151.2, 148.7, 147.9, 141.7, 141.1, 140.4, 139.6, 137.7, 137.4, 136.2, 128.7, 126.7, 126.2, 125.9, 124.9, 121.2, 120.8 (aryl C), 35.9, 30.3 (*t*-Bu), 23.5, 21.3 (CH_3 of Mes). Anal. Calcd for $\text{C}_{78}\text{H}_{74}\text{B}_2\text{F}_{12}\text{N}_6\text{P}_2\text{Ru}$: C, 65.71; H, 6.17; N, 4.85. Found: C, 65.64; H, 6.22; N, 4.83.

X-ray Diffraction Analysis. Single crystals of 3 and 4 were mounted on glass fibers for data collection. Data were collected on a Bruker Apex II single-crystal X-ray diffractometer with graphite-monochromated Mo K α radiation, operating at 50 kV and 30 mA and at 180 K. Data were processed on a personal computer (PC) with the aid of the Bruker SHELXTL software package (version 6.14)¹² and corrected for absorption effects. No significant decay was observed. Crystals of 3 belong to the monoclinic space group $P2_1/n$, while 4 belongs to the triclinic space group $P\bar{1}$. There is one ethylacetate solvent molecule co-crystallized with 3 (one per molecule). Some of the *t*-butyl groups and one of the mesityl groups in 4 display some degrees of rotational disordering, which were not fully addressed, because of the lack of sufficient data.

■ ASSOCIATED CONTENT

S Supporting Information. UV–vis and fluorescent titration data by cyanide ions, binding constant determination, NMR spectra of all complexes, and crystal structural data. This material is available free of charge via the Internet at <http://pubs.acs.org>.

■ AUTHOR INFORMATION

Corresponding Author

*wangs@chem.queensu.ca.

■ ACKNOWLEDGMENT

We thank the Natural Sciences and Engineering Research Council of Canada for financial support, Dr. Rui-Yao Wang for assistance in crystal structural work, and Professor Nick Mosey for DFT computation discussion.

■ REFERENCES

- (1) (a) Yuan, Z.; Taylor, N. J.; Ramachandran, R.; Marder, T. B. *Appl. Organomet. Chem.* **1996**, *10*, 305. (b) Yuan, Z.; Entwistle, C. D.; Collings, J. C.; Albesa-Jové, D.; Batsanov, A. S.; Howard, J. A. K.; Kaiser, H. M.; Kaufmann, D. E.; Poon, S.-Y.; Wong, W.-Y.; Jardin, C.; Fathallah, S.; Boucekkine, A.; Halet, J.-F.; Taylor, N. J.; Marder, T. B. *Chem.—Eur. J.* **2006**, *12*, 2758. (c) Entwistle, C. D.; Marder, T. B. *Angew. Chem., Int. Ed.* **2002**, *41*, 2927. (d) Entwistle, C. D.; Marder, T. B. *Chem. Mater.* **2004**, *16*, 4574. (e) Stahl, R.; Lambert, C.; Kaiser, C.; Wortmann, R.; Jakober, R. *Chem.—Eur. J.* **2006**, *12*, 2358. (f) Matsumi, N.; Chujo, Y. *Polym. J.* **2008**, *40*, 77. (g) Lequan, M.; Lequan, R. M.; Ching, K. C. *J. Mater. Chem.* **1991**, *1*, 997. (h) Liu, Z. Q.; Fang, Q.; Cao, D. X.; Wang, D.; Xu, G. B. *Org. Lett.* **2004**, *6*, 2933. (i) Tao, L. M.; Guo, Y. H.; Huang, X. M.; Wang, C. K. *Chem. Phys. Lett.* **2006**, *425*, 10.

(2) (a) Noda, T.; Shirota, Y. *J. Am. Chem. Soc.* **1998**, *120*, 9714. (b) Shirota, Y. *J. Mater. Chem.* **2005**, *15*, 75. (c) Noda, T.; Ogawa, H.; Shirota, Y. *Adv. Mater.* **1999**, *11*, 283. (d) Shirota, Y.; Kinoshita, M.; Noda, T.; Okumoto, K.; Ohara, T. *J. Am. Chem. Soc.* **2000**, *122*, 1102. (e) Jia, W. L.; Bai, D. R.; McCormick, T.; Liu, Q. D.; Motala, M.; Wang, R.; Seward, C.; Tao, Y.; Wang, S. *Chem.—Eur. J.* **2004**, *10*, 994. (f) Jia, W. L.; Feng, X. D.; Bai, D. R.; Lu, Z. H.; Wang, S.; Vamvounis, G. *Chem. Mater.* **2005**, *17*, 164. (g) Li, F. H.; Jia, W. L.; Wang, S.; Zhao, Y. Q.; Lu, Z. H. *J. Appl. Phys.* **2008**, *103*, 034509/1. (h) Wakamiya, A.; Mori, K.; Yamaguchi, S. *Angew. Chem., Int. Ed.* **2007**, *46*, 4237.

(3) (a) Yamaguchi, S.; Shirasaka, T.; Akiyama, S.; Tamao, K. *J. Am. Chem. Soc.* **2002**, *124*, 8816. (b) Yamaguchi, S.; Akiyama, S.; Tamao, K. *J. Am. Chem. Soc.* **2001**, *123*, 11372. (c) Solé, S.; Gabbai, F. P. *Chem. Commun.* **2004**, 1284. (d) Melaimi, M.; Gabbai, F. P. *J. Am. Chem. Soc.* **2005**, *127*, 9680. (e) Chiu, C. W.; Gabbai, F. P. *J. Am. Chem. Soc.* **2006**, *128*, 14248. (f) Lee, M. H.; Gabbai, F. P. *Inorg. Chem.* **2007**, *46*, 8132. (g) Hudnall, T. W.; Gabbai, F. P. *J. Am. Chem. Soc.* **2007**, *129*, 11978. (h) Hudnall, T. W.; Kim, Y.-M.; Bebbington, M. W. P.; Bourissou, D.; Gabbai, F. P. *J. Am. Chem. Soc.* **2008**, *130*, 10890. (i) Wade, C. R.; Broomsgrove, A. E. J.; Aldridge, S.; Gabbai, F. P. *Chem. Rev.* **2010**, *110*, 3958, and references therein.

(4) (a) Sundararaman, A.; Venkatasubbaiah, K.; Victor, M.; Zakharov, L. N.; Rheingold, A. L.; Jäkle, F. *J. Am. Chem. Soc.* **2006**, *128*, 16554. (b) Parab, K.; Venkatasubbaiah, K.; Jäkle, F. *J. Am. Chem. Soc.* **2006**, *128*, 12879. (c) Lorbach, A.; Bolte, M.; Li, H.; Lerner, H.-W.; Holthausen, M. C.; Jäkle, F.; Wagner, M. *Angew. Chem., Int. Ed.* **2009**, *48*, 4584. (d) Jäkle, F. *Coord. Chem. Rev.* **2006**, *250*, 1107. (e) Jäkle, F. *Chem. Rev.* **2010**, *110*, 3985, and references therein. (f) Liu, X. Y.; Bai, D. R.; Wang, S. *Angew. Chem., Int. Ed.* **2006**, *45*, 5475. (g) Bai, D. R.; Liu, X. Y.; Wang, S. *Chem.—Eur. J.* **2007**, *13*, 5713. (h) Zhao, S. B.; Wucher, P.; Hudson, Z. M.; McCormick, T. M.; Liu, X. Y.; Wang, S.; Feng, X. D.; Lu, Z. H. *Organometallics* **2008**, *27*, 6446. (i) Zhou, G.; Baumgarten, M.; Müllen, K. *J. Am. Chem. Soc.* **2008**, *130*, 12477.

(5) (a) Sun, Y.; Ross, N.; Zhao, S. B.; Huszarik, K.; Jia, W. L.; Wang, R. Y.; Wang, S. *J. Am. Chem. Soc.* **2007**, *129*, 7510. (b) Sun, Y.; Wang, S. *Inorg. Chem.* **2009**, *48*, 3755. (c) Sun, Y.; Wang, S. *Inorg. Chem.* **2010**, *49*, 4394. (d) Rao, Y. L.; Wang, S. *Inorg. Chem.* **2009**, *48*, 7698.

(6) (a) Sakuda, E.; Funahashi, A.; Kitamura, N. *Inorg. Chem.* **2006**, *45*, 10670. (b) Zhao, Q.; Li, F. Y.; Liu, S. J.; Yu, M. X.; Liu, Z. Q.; Yi, T.; Huang, C. H. *Inorg. Chem.* **2008**, *47*, 9256. (c) Lam, S. T.; Zhu, N.; Yam, V. W. W. *Inorg. Chem.* **2009**, *48*, 9664. (d) You, Y.; Park, S. Y. *Dalton Trans.* **2009**, 1267. (e) Day, J. K.; Bresner, C.; Coombs, N. D.; Fallis, I. A.; Ooi, L. L.; Aldridge, S. *Inorg. Chem.* **2008**, *47*, 793. (f) Wade, C. R.; Gabbai, F. P. *Inorg. Chem.* **2010**, *49*, 714.

(7) (a) Zhao, S. B.; McCormick, T.; Wang, S. *Inorg. Chem.* **2007**, *46*, 10965. (b) Hudson, Z. M.; Zhao, S. B.; Wang, S. *Chem.—Eur. J.* **2009**, *15*, 6081. (c) Hudson, Z. M.; Sun, C.; Helander, M. G.; Amarne, H.; Lu, Z. H.; Wang, S. *Adv. Funct. Mater.* **2010**, *20*, 3426. (d) Zhou, G. J.; Ho, C. L.; Wong, W. Y.; Wang, Q.; Ma, D. G.; Wang, L. X.; Lin, Z. Y.; Marder, T. B.; Beeby, A. *Adv. Funct. Mater.* **2008**, *18*, 499.

(8) (a) Juris, A.; Balzani, V.; Barigelletti, F.; Campagna, S.; Belser, P.; von Zelewsky, A. *Coord. Chem.* **1988**, *84*, 85. (b) Balzani, V.; Juris, A.; Venturi, M.; Campagna, S.; Serroni, S. *Chem. Rev.* **1996**, *96*, 759. (c) Sauvage, J. P.; Collin, J. P.; Chambron, J. C.; Guillerez, S.; Coudret, C.; Balzani, V.; Barigelletti, F.; De Cola, L.; Flamigni, L. *Chem. Rev.* **1994**, *94*, 993.

(9) Caspar, J. V.; Meyer, T. J. *J. Am. Chem. Soc.* **1983**, *105*, 5583.

(10) Kasha, M. *Discuss. Faraday Soc.* **1950**, *9*, 14.

(11) For example, see: (a) Caspar, R.; Cordier, C.; Waern, J. B.; Guyard-Duhayon, C.; Gruselle, M.; Le Floch, P.; Amouri, H. *Inorg. Chem.* **2006**, *45*, 4071. (b) Jose, D. A.; Kar, P.; Koley, D.; Ganguly, B.; Thiel, W.; Ghosh, H. N.; Das, A. *Inorg. Chem.* **2007**, *46*, 5576.

(12) *SHELXTL Version 6.14*; Bruker AXS: Madison, WI, 2000–2003.